

## Observation of the Undercoolability of Quasicrystal-Forming Alloys by Electromagnetic Levitation

D. Holland-Moritz,<sup>1,2</sup> D. M. Herlach,<sup>1</sup> and K. Urban<sup>2</sup>

<sup>1</sup>*Institut für Raumsimulation, Deutsche Forschungsanstalt für Luft- und Raumfahrt, D-51140 Köln, Germany*

<sup>2</sup>*Forschungszentrum Jülich, Institut für Festkörperforschung, D-5170 Jülich, Germany*

(Received 8 March 1993)

The electromagnetic levitation technique is applied to undercool melts of quasicrystal-forming alloys of Al-Cu-Co and Al-Cu-Fe. Undercooling with respect to the solidification of the decagonal phase (quasiperiodic in two dimensions) and the icosahedral phase (quasiperiodic in three dimensions) is measured *in situ* by contactless temperature measurements. The undercoolings are analyzed within nucleation theory. The results indicate that the activation energy for the formation of the nuclei of quasicrystalline phases is lower than that of crystalline phases. The decrease of activation energy is more pronounced for the icosahedral phase than for the decagonal phase.

PACS numbers: 64.70.Dv, 61.25.Mv, 61.44.+p, 81.30.Fb

Following the pioneering work by Turnbull [1], it is now well established that metallic melts can be substantially undercooled below the solid melting temperature. A relative undercooling of  $\Delta T/T_L$  ( $T_L$  is the melting or liquidus temperature) on the order of 20% has been found for a series of different metallic elements. Frank [2] pointed out that such high undercoolings may be caused by an icosahedral short range order (ISRO) in the undercooled liquid. A characteristic feature of ISRO is fivefold rotational symmetry which is incompatible with the translational symmetry of normal crystalline phases. This may give rise to an additional barrier for the nucleation of crystalline phases, since the ISRO must be broken before solidification of crystalline phases can occur. Computer simulation experiments on simple Lennard-Jones liquids confirmed that ISRO should be energetically favored in the undercooled melt [3]. Further evidence for this assumption comes from the identification of magic numbers in the mass spectra of free atomic cluster beams with numbers of atoms of 13, 55, 147, . . . corresponding to icosahedral aggregates [4]. However, the dense packing of atoms in icosahedrally ordered atomic aggregates also implies the phenomenon of space frustration, which progressively increases with increasing cluster size and consumes the energy gain by the icosahedral packing at a critical cluster size. High-resolution electron microscopy studies on Au clusters show phase fluctuations between icosahedral and fcc ordering at cluster sizes of about 600 atoms [5]. This may indicate that at such a cluster size the effect of energy gain due to icosahedral ordering is compensated by the energy loss due to the effect of space frustration.

According to classical nucleation theory, one expects cluster sizes for the formation of critical nuclei in liquids on the order of a few hundred atoms [6]. Therefore, the question arises whether ISRO in undercooled melts may favor large undercoolings or not. This question attracted renewed attention after the discovery of the new class of quasicrystalline materials [7]. The short range order in quasicrystalline phases is quite similar to that of an

icosahedron. From this point of view one expects that the nucleation of quasicrystalline phases may be favored by an ISRO in the undercooled melt, leading to a reduction of the relative undercooling. So far, only indirect investigations of undercooling and nucleation of quasicrystalline phases in Al-Mn alloys have been reported [8].

In the present work we report on the first direct measurements of the undercooling of the decagonal (*D*) phase in  $\text{Al}_{65}\text{Cu}_{25}\text{Co}_{10}$  and the icosahedral (*I*) phase in  $\text{Al}_{60}\text{Cu}_{34}\text{Fe}_6$  alloys. These alloys were selected since they form quasicrystalline phases even at moderate cooling rates [9]. The alloy compositions were chosen after detailed preinvestigations had shown that primary solidification of quasicrystalline phases is ensured [10]. This is essential for the interpretation of the undercooling results. The samples were prepared by inductively premelting the constituents, all of purity better than 99.999%, in a water-cooled Cu crucible under an Ar gas atmosphere. Undercooling conditions were established by the electromagnetic levitation technique which allows containerless processing of samples of about 7 mm in diameter in an He-10%  $\text{H}_2$  gas environment. Direct measurements of temperature-time profiles during heating, cooling, undercooling, and solidification of the levitated drop were performed by a pyrometer (accuracy  $\pm 10$  K, sampling rate of 100 Hz). Further details of the levitation chamber are given elsewhere [10]. The as-solidified samples were examined by scanning (SEM) and transmission (TEM) electron microscopy. In addition, differential-thermal analysis (DTA) was used to determine the liquidus and transformation temperatures of the alloys.

The application of the electromagnetic levitation technique guarantees the avoidance of container-wall induced heterogeneous nucleation. As a consequence, undercoolings can be achieved on the order of  $\Delta T/T_L \approx 0.20$  for bulk samples of pure metals which are otherwise only obtainable by the droplet dispersion technique on small particles [11]. All the samples were undercooled several times. The reproducibility of the undercooling results is better than  $\pm 10$  K. Figure 1 shows a temperature-time

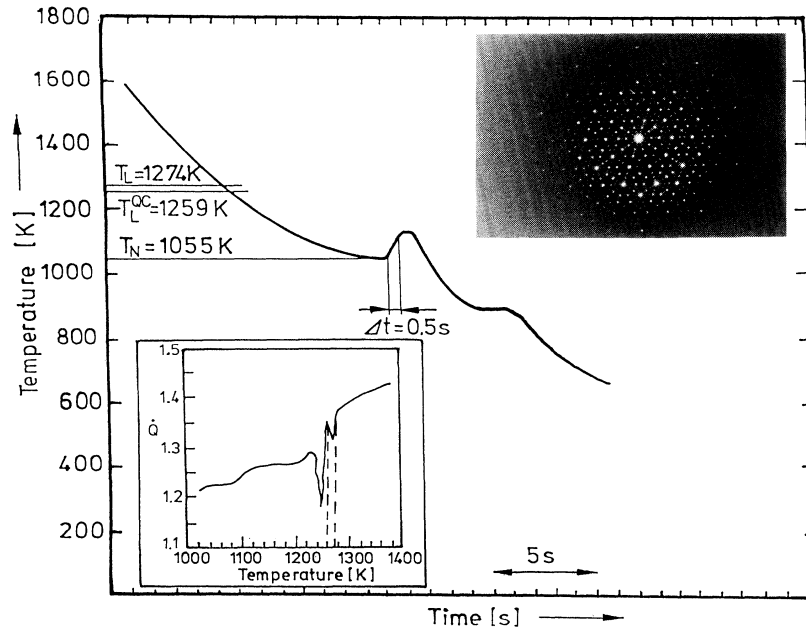


FIG. 1. Temperature-time profile as obtained from a bulk  $\text{Al}_{65}\text{Cu}_{25}\text{Co}_{10}$  melt solidified in the containerless state. The inset on the right-hand side shows a TEM diffraction pattern of the as-solidified sample. The inset on the left-hand side gives a DTA trace.

profile obtained for  $\text{Al}_{65}\text{Cu}_{25}\text{Co}_{10}$ . Here, the sample is undercooled to  $\Delta T = 205$  K with respect to the melting temperature of the quasicrystalline phase. This corresponds to a relative undercooling of  $\Delta T/T_L = 0.16$ . The release of the heat of transformation leads to a temperature rise during recalescence. The recalescence time  $\tau$  amounts to 0.5 s. Taking into account the measuring area of the pyrometer (diameter  $d = 0.34$  cm), the solidification velocity can be estimated from  $V = d/\tau$  to be  $V \approx 0.7$  cm/s. This is much less than measured for pure metals and simple alloys [12]. The inset on the left-hand side gives a DTA trace during cooling for the same alloy, from which the liquidus temperature of the quasicrystalline  $D$  phase is inferred. The inset on the right-hand side shows a TEM pattern of the as-solidified sample giving evidence that the quasicrystalline  $D$  phase solidified.

Figure 2 represents an equivalent temperature-time profile obtained for  $\text{Al}_{60}\text{Cu}_{34}\text{Fe}_6$ . In comparison to the  $\text{Al}_{65}\text{Cu}_{25}\text{Co}_{10}$  alloy, the undercooling is smaller and amounts to  $\Delta T = 110$  K or  $\Delta T/T_L = 0.10$  with respect to the melting temperature of the quasicrystalline  $I$  phase. The recalescence time is  $t = 0.7$  s, indicating a smaller solidification velocity of the  $I$  phase of  $V \approx 0.5$  cm/s. The TEM pattern (inset on the right-hand side) reveals solidification of the  $I$  phase. The DTA trace (inset on the left-hand side) provides the liquidus temperature of the  $I$  phase. All data inferred from Figs. 1 and 2 are collected in Table I.

For further analysis it is important to identify the primary phase formed after undercooling. Figure 3 shows

the microstructure (obtained by SEM) of the as-solidified sample of  $\text{Al}_{60}\text{Cu}_{34}\text{Fe}_6$  [13]. Primary solidification of the icosahedral phase (1) is indicated by the formation of dendrites (note that the formation of dendrites always needs undercooling [12]), which is followed by the formation of a phase of Cs-Cl type structure (2), intermetallic  $\text{Al}_2\text{Cu}$  (3), and  $\text{AlCu}$  (4). It is noteworthy that due to the large undercoolings the crystallization of the  $\lambda$  phase ( $\text{Al}_{13}\text{Fe}_4$ ) is circumvented, which otherwise crystallizes at small undercoolings. Equivalent investigations on the Al-Cu-Co alloy show a similar microstructure evolution, however, with the  $D$  phase primary solidified.

For the interpretation of the experimental results we refer to classical nucleation theory [6]. The steady-state homogeneous nucleation rate  $I_{ss}$  is given by

$$I_{ss} = [k_B T N_L / 3 \eta(T) a_0^3] \exp(-\Delta G^* / k_B T), \quad (1)$$

with

$$\Delta G^* = 16\pi\sigma^3 / 3\Delta G^2.$$

$a_0$  is an interatomic spacing and  $\eta(T)$  is the viscosity of the undercooled melt.  $N_L$  denotes Avogadro's number and  $k_B$  is Boltzmann's constant.  $\Delta G^*$  is the activation threshold for the formation of a critical nucleus with  $\sigma$  being the interfacial energy of the solid-liquid interface and  $\Delta G$  the difference of the Gibbs free energy between solid and liquid. The temperature dependence of the viscosity of quasicrystal-forming alloy melts can be approximated by a Vogel-Fulcher ansatz [14],

$$\eta(T) = \eta_0 \exp[A / (T - T_0)]. \quad (2)$$

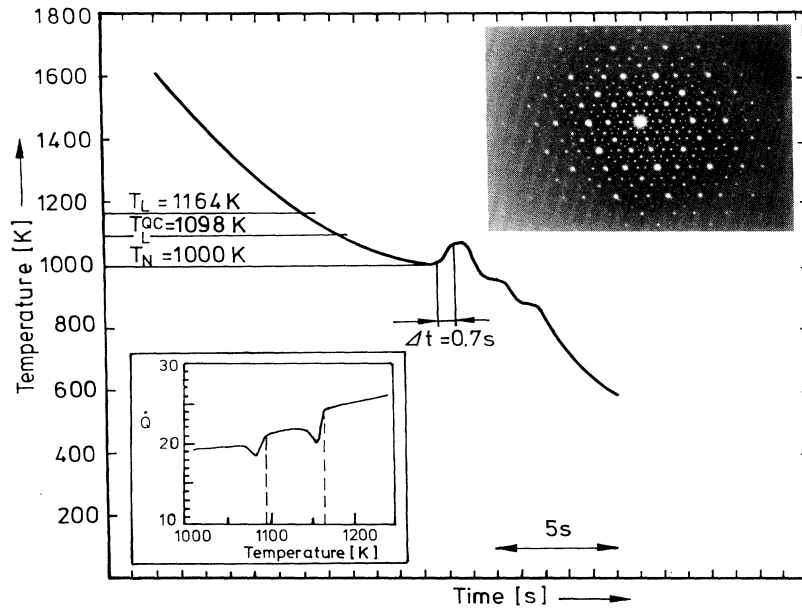


FIG. 2. Temperature-time profile as obtained from a bulk  $\text{Al}_{60}\text{Cu}_{34}\text{Fe}_6$  melt solidified in the containerless state. The inset on the right-hand side shows a TEM diffraction pattern of the as-solidified sample. The inset on the left-hand side gives a DTA trace.

For an estimate we assume that the value of parameter  $A$  is the same as for Al-Mn [8]. The prefactor  $\eta_0$  is calculated such that  $\eta(T_L) = 1$  P, as is typical of quasicrystal-forming alloys.  $T_0$  corresponds to the ideal glass transition temperature. We use  $T_0 = 0.5T_L$  for a first approximation. The Gibbs free energy difference is calculated according to an expression shown to be a good approximation for Al-Mn alloys [8],

$$\Delta G = \Delta S_f \Delta T - \gamma \Delta S_f \left[ \Delta T - T \ln \left( \frac{T_L}{T} \right) \right], \quad (3)$$

with  $\gamma = [\ln(T_L/T_0)]^{-1}$  a proportional constant and  $\Delta S_f$  the entropy of fusion [15]. To estimate the interfacial energy  $\sigma$ , we refer to the negentropic model developed by Spaepen [16] and Thompson [17],

$$\sigma = \alpha \Delta S_f T / (N_L V_m^2)^{1/3}, \quad (4)$$

where  $\alpha$  is a factor depending on the structure of the solid nucleus ( $\alpha = 0.86$  for fcc and  $\alpha = 0.71$  for bcc), and  $V_m$  is the molar volume. The negentropic model assumes tetrahedral short range order in the interface which has a similarity with the short range order of quasicrystals. Taking into account Eq. (1) and using the values for the different parameters as listed in Table I, the experimentally determined values of the maximum undercooling are analyzed with  $\alpha$  being the only fit parameter.  $\alpha$  reflects

TABLE I. Characteristic thermodynamic data used for the calculations of the nucleation behavior of the undercooled melt into quasicrystalline decagonal ( $\text{Al}_{65}\text{Cu}_{25}\text{Co}_{10}$ ) and icosahedral ( $\text{Al}_{60}\text{Cu}_{34}\text{Fe}_6$ ) phases, respectively.

Parameter	Units	$\text{Al}_{65}\text{Cu}_{25}\text{Co}_{10}$	$\text{Al}_{60}\text{Cu}_{34}\text{Fe}_6$
Melting temperatures of quasicrystalline phases	K	1259	1098
Molar volume	$\text{m}^3/\text{mol}$	$8.3 \times 10^{-6}$	$8.3 \times 10^{-6}$
Entropy of fusion	$\text{J}/(\text{K mol})$	8.45	8.42
$A$	K	2106	2106
$\eta_0$	P	0.0352	0.0216
Mass density	$\text{g}/\text{cm}^3$	4.6	4.6

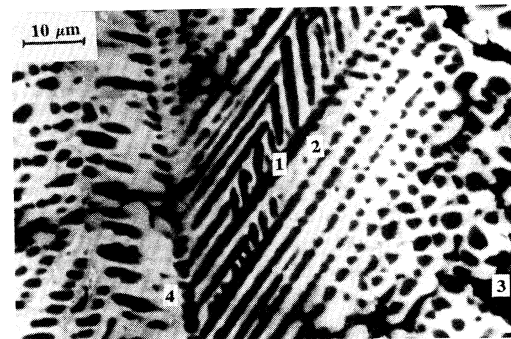


FIG. 3. Microstructure of the as-solidified sample of  $\text{Al}_{60}\text{Cu}_{34}\text{Fe}_6$ . The following phases are identified: the  $I$  phase (1) of composition  $\text{Al}_{64.4}\text{Cu}_{22.6}\text{Fe}_{13}$ , primary solidified, a phase of Cs-Cl type structure (2) of composition  $\text{Al}_{57.5}\text{Cu}_{36.3}\text{Fe}_{6.2}$ , intermetallic  $\text{Al}_2\text{Cu}$  (3), and  $\text{AlCu}$  (4).

the most important influence of the structure of the solid nucleus on nucleation behavior and is determined quantitatively on the basis of the measured undercoolings for the *D* and *I* phases, respectively. For the further analysis it is assumed that at least one nucleation event is necessary to initiate solidification of the undercooled melt so that  $I_{ss}Vt=1$ .  $V$  denotes the volume of the sample and  $t$  gives the experiment time  $t=(T_L-T_n)/(dT/dt)$  with  $T_n$  the nucleation temperature and  $dT/dt$  the cooling rate. Both quantities are inferred from the corresponding temperature-time profiles. This analysis leads to the conclusion that  $\alpha=0.47$  for the *D* phase and  $\alpha=0.32$  for the *I* phase.

Our analysis is based upon the assumption of *homogeneous* nucleation and suggests a low interfacial energy between quasicrystalline nucleus and undercooled melt. This is in agreement with results of the investigation of the kinetics of icosahedral phase formation upon heat treatment of rapidly quenched Al-Mn [18]. In addition, atomization experiments on Al-Mn revealed an extremely high density of quasicrystalline particles, on the order of  $10^{18} \text{ cm}^{-3}$ , which has been interpreted as an indication for homogeneous nucleation [19]. On the basis of these and additional experiments in a drop tube temperature-time-transformation (TTT) diagrams were calculated anticipating homogeneous nucleation [8]. For the cooling rates occurring in the present experiments undercoolings are predicted by these diagrams which are comparable to those measured. All these observations confirm that the assumption of homogeneous nucleation is justified. If, nevertheless, heterogeneous nucleation is tentatively assumed this would have the following consequences: Anticipating the same catalytic potency  $f(\theta)$  for all phases our main conclusions remain unchanged, i.e., that the interfacial energy of the quasicrystalline phases is lower than that of crystalline phases and that it decreases when going from a decagonal to icosahedral structure. On the other hand, if the observed change of  $\Delta G^*$  is exclusively attributed to a change in  $f(\theta)$  an anomalous variation has to be postulated, i.e., by a factor of 3 between the two quasicrystalline phases and even higher values between the icosahedral and crystalline phases.

In summary, the electromagnetic levitation processing of quasicrystal-forming alloys of  $\text{Al}_{65}\text{Cu}_{25}\text{Co}_{10}$  and  $\text{Al}_{60}\text{Cu}_{34}\text{Fe}_6$  was applied to measure undercoolings of quasicrystal decagonal and icosahedral phases. The analysis of the results within the classical nucleation theory leads to the conclusion that the activation threshold  $\Delta G^*$  for the nucleation of quasicrystalline phases is smaller than that for crystalline phases. Further direct

support for this finding comes from the observation that primary crystallization of competing crystalline phases (of even higher melting temperatures than those of the quasicrystalline phases) can be circumvented. This result is explained by an ISRO in the undercooled melt and is in agreement with an analysis of short range order in undercooled liquids [20].

Financial support for the present work by the Deutsche Agentur für Raumfahrtangelegenheiten (DARA) is gratefully acknowledged.

- 
- [1] D. Turnbull, *J. Appl. Phys.* **21**, 1022 (1950).
  - [2] F. C. Frank, *Proc. R. Soc. London A* **215**, 43 (1952).
  - [3] P. J. Steinhardt, D. R. Nelson, and M. Ronchetti, *Phys. Rev. B* **28**, 784 (1983).
  - [4] K. Sattler, J. Mühlbach, O. Echt, P. Pfau, and E. Recknagel, *Phys. Rev. Lett.* **47**, 160 (1981).
  - [5] S. Jijima and T. Ichihashi, *Phys. Rev. Lett.* **56**, 616 (1986).
  - [6] J. W. Christian, *The Theory of Transformation in Metals and Alloys* (Pergamon, Oxford, 1975).
  - [7] D. Shechtman, I. Blech, D. Gratias, and J. Cahn, *Phys. Rev. Lett.* **53**, 1951 (1984).
  - [8] D. M. Herlach, F. Gillessen, T. Volkman, M. Wollgarten, and K. Urban, *Phys. Rev. B* **46**, 5203 (1992).
  - [9] A. P. Tsai, A. Inoue, and T. Masumoto, *Jpn. J. Appl. Phys.* **26**, L1505 (1987).
  - [10] D. Holland-Moritz, D. M. Herlach, and K. Urban (to be published).
  - [11] D. M. Herlach and R. Willnecker, in *Rapidly Solidified Alloys*, edited by H. H. Liebermann (Marcel Dekker, New York, 1993), p. 79.
  - [12] R. Willnecker, D. M. Herlach, and B. Feuerbacher, *Phys. Rev. Lett.* **62**, 2707 (1989).
  - [13] Structure formation under equilibrium conditions in ternary Al-Cu-Co and Al-Cu-Fe alloys as a function of concentration has been analyzed in detail by B. Grushko.
  - [14] L. Battezzati, C. Antonione, and F. Marino, *J. Mater. Sci.* **24**, 2324 (1989).
  - [15] F. Gillessen and D. M. Herlach, *Mater. Sci. Eng. A* **134**, 1220 (1991).
  - [16] F. Spaepen, *Acta Metall.* **23**, 729 (1975).
  - [17] C. V. Thompson, Ph.D. thesis, Harvard University, 1979.
  - [18] K. F. Kelton and J. C. Holzer, *Phys. Rev. B* **37**, 3940 (1988).
  - [19] L. A. Bendersky and S. D. Ridder, *J. Mater. Res.* **1**, 405 (1986).
  - [20] D. R. Nelson and F. Spaepen, *Solid State Physics*, edited by H. Ehrenreich, F. Seitz, and D. Turnbull (Academic, New York, 1989), Vol. 42, p. 1.

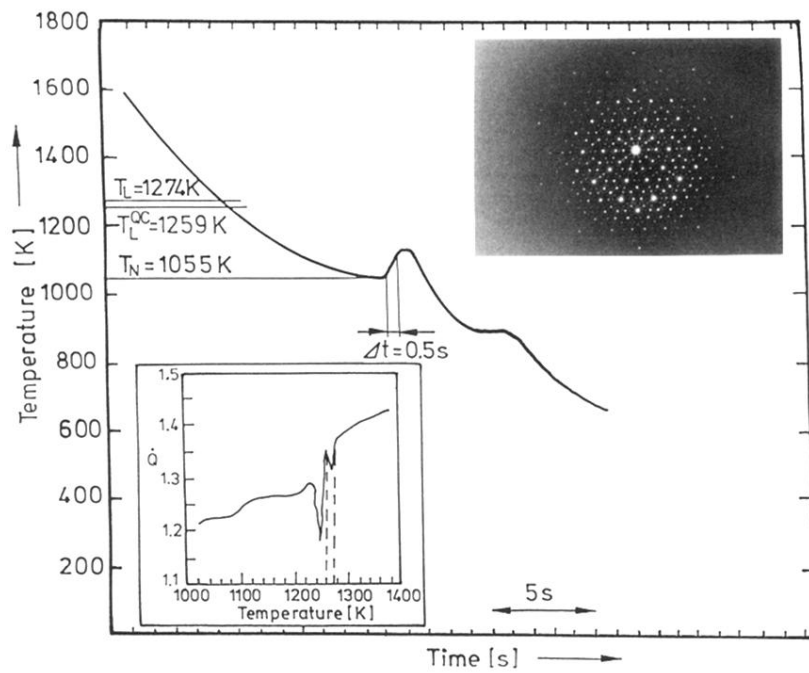


FIG. 1. Temperature-time profile as obtained from a bulk  $\text{Al}_{65}\text{Cu}_{25}\text{Co}_{10}$  melt solidified in the containerless state. The inset on the right-hand side shows a TEM diffraction pattern of the as-solidified sample. The inset on the left-hand side gives a DTA trace.

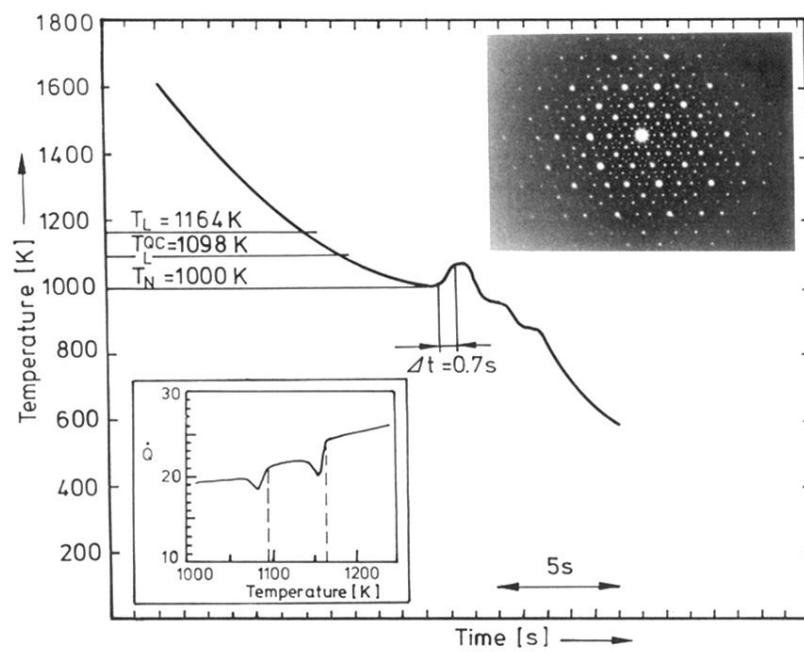


FIG. 2. Temperature-time profile as obtained from a bulk  $\text{Al}_{60}\text{Cu}_{34}\text{Fe}_6$  melt solidified in the containerless state. The inset on the right-hand side shows a TEM diffraction pattern of the as-solidified sample. The inset on the left-hand side gives a DTA trace.

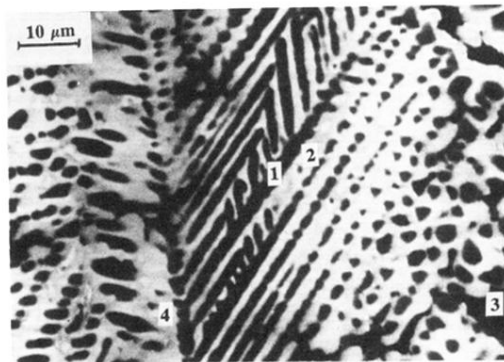


FIG. 3. Microstructure of the as-solidified sample of  $\text{Al}_{60}\text{Cu}_{34}\text{Fe}_6$ . The following phases are identified: the  $I$  phase (1) of composition  $\text{Al}_{64.4}\text{Cu}_{22.6}\text{Fe}_{13}$ , primary solidified, a phase of Cs-Cl type structure (2) of composition  $\text{Al}_{57.5}\text{Cu}_{36.3}\text{Fe}_{6.2}$ , intermetallic  $\text{Al}_2\text{Cu}$  (3), and  $\text{AlCu}$  (4).